Evolution of Genomic and T-cell Repertoire Heterogeneity of Malignant Pleural Mesothelioma Under Dasatinib Treatment

Runzhe Chen[1,2], Won-Chul Lee[2], Junya Fujimoto[3], Jun Li[2], Xin Hu[2], Reza Mehran[4], David Rice[4], Stephen G. Swisher[4], Boris Sepesi[4], Hai T. Tran[1], Chi-Wan Chow[3], Latasha D. Little[2], Curtis Gumbs[2], Cara Haymaker[3], John V. Heymach[1], Ignacio I. Wistuba[3], J. Jack Lee[5], P. Andrew Futreal[2], Jianhua Zhang[2], Alexandre Reuben[1], Anne S. Tsao[1], and Jianjun Zhang[1,2]

ABSTRACT

Purpose: Malignant pleural mesothelioma (MPM) is considered an orphan disease with few treatment options. Despite multimodality therapy, the majority of MPMs recur and eventually become refractory to any systemic treatment. One potential mechanism underlying therapeutic resistance may be intratumor heterogeneity (ITH), making MPM challenging to eradicate. However, the ITH architecture of MPM and its clinical impact have not been well studied.

Experimental Design: We delineated the immunogenomic ITH by multiregion whole-exome sequencing and T-cell receptor (TCR) sequencing of 69 longitudinal MPM specimens from nine patients with resectable MPM, who were treated with dasatinib.

Results: The median total mutation burden before dasatinib treatment was 0.65/Mb, similar with that of post-dasatinib treatment (0.62/Mb). The median proportion of mutations shared by any given pair of two tumor regions within the same tumors was 80% prior to and 83% post-dasatinib treatment indicating a relatively homogenous genomic landscape. T-cell clonality, a parameter indicating T-cell expansion and reactivity, was significantly increased in tumors after dasatinib treatment. Furthermore, on average, 82% of T-cell clones were restricted to individual tumor regions, with merely 6% of T-cell clones shared by all regions from the same tumors indicating profound TCR heterogeneity. Interestingly, patients with higher T-cell clonality and higher portion of T cells present across all tumor regions in post-dasatinib–treated tumors had significantly longer survival.

Conclusions: Despite the homogeneous genomic landscape, the TCR repertoire is extremely heterogeneous in MPM. Dasatinib may potentially induce T-cell response leading to improved survival.

Introduction

Malignant pleural mesothelioma (MPM) is a rare and highly aggressive malignancy characterized by unique morphology that commonly grows as an irregular pleural rind within the affected hemithorax (1, 2). MPM is often refractory to aggressive multimodality therapy, combining surgery with chemo- and/or radiotherapy. Recent studies from patients with MPM carrying germline mutations in tumor suppressor genes such as *BAP1* or DNA repair genes have shown improved survival results (3, 4). However, despite significant efforts to develop novel therapeutics, the median survival of patients with MPM still remains between 12 and 18 months with a 5-year overall survival (OS) rate less than 5%, regardless of stage (2, 5–7). Understanding the mechanisms underlying therapeutic resistance of MPM remains a critical and largely unmet need.

One potential mechanism underlying the aggressiveness and therapeutic resistance in malignancy is intratumor heterogeneity (ITH), wherein different cancer cell clones with distinct molecular and phenotypic features are present within the same tumors, leading to differential responses to treatment (8–12). ITH has been found to associate with therapeutic resistance and survival of patients with different cancer types (8–12). Using a multiregion sequencing approach, our group and others have previously delineated the genomic, epigenetic, and transcriptomic ITH architecture of non–small cell lung cancers (NSCLCs) and demonstrated that complex molecular ITH was associated with inferior clinical outcomes (13–19). Given the unique growth pattern of MPM (wide spreading irregular pleural rind across pleura) compared with most other solid tumors (growing as a solid mass), MPM may have profound ITH, which makes it challenging to eradicate by currently available therapeutic modalities.

In addition to ITH of cancer cells, ITH can also be present in the tumor microenvironment, particularly cancer immune contexture, which may have significant impact on cancer biology and clinical outcome. Our recent work has revealed substantial T-cell receptor (TCR) repertoire heterogeneity in localized NSCLC, which was associated with inferior survival (15). Investigating the molecular and immune ITH architecture of MPM and its evolution under therapy may provide novel insight into the mechanisms underlying therapeutic

[1]Department of Thoracic/Head and Neck Medical Oncology, The University of Texas MD Anderson Cancer Center, Houston, Texas. [2]Department of Genomic Medicine, The University of Texas MD Anderson Cancer Center, Houston, Texas. [3]Department of Translational Molecular Pathology, The University of Texas MD Anderson Cancer Center, Houston, Texas. [4]Department of Thoracic and Cardiovascular Surgery, The University of Texas MD Anderson Cancer Center, Houston, Texas. [5]Department of Biostatistics, The University of Texas MD Anderson Cancer Center, Houston, Texas.

Note: Supplementary data for this article are available at Clinical Cancer Research Online (http://clincancerres.aacrjournals.org/).

R. Chen and W.-C. Lee contributed equally to this article.

A.S. Tsao and J. Zhang co-supervised this article.

Corresponding Authors: Jianjun Zhang, The University of Texas MD Anderson Cancer Center, Unit 432, 1515 Holcombe Blvd, Houston, TX 77030. Phone: 713-792-6363; E-mail: JZhang20@mdanderson.org; and Anne S. Tsao, Departments of Thoracic and Head and Neck Medical Oncology, The University of Texas MD Anderson Cancer Center. Phone: 713-792-6363; E-mail: astsao@mdanderson.org

Clin Cancer Res 2020;26:5477–86

doi: 10.1158/1078-0432.CCR-20-1767

Translational Relevance

Malignant pleural mesothelioma (MPM) is a rare and highly aggressive malignancy. MPM was believed to have profound intratumor heterogeneity (ITH), which makes it challenging to eradicate. In this study, we delineated the genomic and T-cell repertoire ITH landscape by multiregion whole-exome sequencing and T-cell receptor (TCR) sequencing of 69 MPM specimens from nine patients with resectable MPM, who were treated with preoperative dasatinib on a neoadjuvant trial. Our results demonstrated a relatively homogenous genomic landscape and extremely heterogeneous TCR repertoire of MPM tumors. T-cell clonality significantly increased after treatment with dasatinib, and patients with higher T-cell clonality and more homogeneous T-cell repertoire in post-dasatinib–treated MPM tumors had significantly longer survival. These findings suggest that dasatinib may induce expansion and reactivation of T cells, therefore, could potentially serve as an immunomodulator to enhance the efficacy of immunotherapy in patients with MPM.

resistance and disease progression. In this study, we performed multiregion whole-exome sequencing (WES) and TCR sequencing of 69 MPM specimens from nine patients with resectable MPM, who were treated with the Src kinase inhibitor, dasatinib, for 4 weeks prior to surgical resection in a neoadjuvant clinical trial protocol 2006-0935 (NCT00652574; refs. 6, 20). These longitudinal specimens included 24 baseline specimens before dasatinib treatment and 45 post-dasatinib treatment.

Materials and Methods

Patients and sample collection

A total of 69 tumor regions consisting of 24 pretreatment samples (two to four regions per tumor) and 45 post-dasatinib samples (three to six regions per tumor) and their matched peripheral blood samples were collected from nine patients with MPM. All patients were treated at the University of Texas MD Anderson Cancer Center (Houston, TX) from 2008 to 2012 on protocol 2006-0935 (NCT00652574; Supplementary Table S1). Prior to dasatinib treatment, patients with MPM underwent extended surgical staging with multiple biopsies of the primary pleural tumor to account for tumor heterogeneity. Each tumor biopsy removed from the patient was cut in half with one part flash frozen and the second part formalin fixed for paraffin (6). Surgical specimens were snap frozen in liquid nitrogen immediately after surgical resection and stored at −80°C. All surgical specimens were identified and collected by surgeons per protocol 2006-0935 and submitted to pathologists for multiregional sampling. All the selected samples for this analysis were subjected to pathologic examination to confirm the diagnosis and ensure the sample quality before DNA extraction. Peripheral blood mononuclear cells were immediately isolated from 10-mL whole blood and stored at −80°C. Written informed consent was obtained from all patients included in the study. The study was approved by the Institutional Review Board at University of Texas MD Anderson Cancer Center (Houston, TX). The study was conducted in accordance with U.S. Common Rule.

WES

Genomic DNA was extracted and subjected to library preparation for sequencing with Agilent SureSelect Human All Exon V4 Kit according to the manufacturer's instructions. The 76-bp paired-end WES was performed on Illumina HiSeq 2000 Platform with mean target coverages of 200× and 100× for tumor and normal samples, respectively, as described previously (14).

Somatic mutation calling

Somatic single-nucleotide variants (SNVs) and somatic small insertions and deletions (INDELs) were called using MuTect (21) and Pindel (22), respectively. Mutations previously reported in public database (dbSNP138, 1000Genomes, ESP6500, and EXAC) with >1% allele frequency were removed. Next, we applied the following mutation-filtering criteria: (i) sequencing depth ≥ 50 for tumor and ≥30 for normal, (ii) tumor allele frequency ≥ 5% for SNVs and ≥10% for INDELs, and (iii) normal allele frequency < 1%.

Mutational signature analysis

Mutation signatures were determined by deconstructSigs (23) with 30 Catalogue of Somatic Mutations in Cancer (COSMIC) signatures provided by the package.

Somatic copy-number aberration analysis

Somatic copy-number aberration (SCNA) analysis was done using our in-house SCNA caller, "exomecn" as described previously (14). The "exomecn" is a modified version of HMMcopy (24). Briefly, it calculates read counts of each exon and then calculates $\log_2$ratios between tumor and matched normal reference samples by considering the total number of reads as a normalization factor. The resulting normalized $\log_2$ratios were segmented using circular binary segmentation algorithm implemented in the DNAcopy package of Bioconductor. The copy ratios of segments were then assigned to the overlapping genes by CNTools (25). We defined copy-number gains and losses in all tumor samples using $+\log_2 1.5$ for gain and $-\log_2 1.5$ for loss, respectively. Because the signal to noise ratio of SCNA could be reduced in the samples with lower tumor purity, we obtained purity-adjusted $\log_2$ ratios by $\log_2$ ((original copy ratio − 1)/purity + 1) (26), if any of the paired samples from the same patients passed the original $\log_2$ thresholds of $+\log_2 1.5$ and $-\log_2 1.5$. Tumor purity was estimated by Sequenza (27). Copy-number gain and loss burden were defined as the number of copy-number gains and losses in a given sample, and the total copy-number burden was a sum of gains and losses.

Phylogeny inference

To infer phylogenetic trees, mutation data were converted to the binary data with mutations being 1 and wild-type being 0 and fed into Phangorn R package. Tree topologies were estimated by *pratchet* and branch lengths were inferred by *acctran*.

Neoantigen prediction

Neoantigens were predicted by NeoPredPipe (28) that uses ANNOVAR and netMHCpan. The SNVs and INDELs were fed into the program with patient-specific HLA types genotyped by HLA-VBSeq (29). Both strong and weak binders were considered predicted neoantigen peptides. The SNVs or INDELs that generated multiple neoantigen peptides with different k-mer settings were only counted once. Trunk neoantigens were defined as predicted neoantigens shared by all the regions per tumor.

TCRβ sequencing and comparison parameters

Sequencing of the CDR3 regions of human TCRβ chains was performed using the protocol of ImmunoSeq (Adaptive Biotechnologies, hsTCRβ Kit) as described previously (15, 30). T-cell density was

calculated by normalizing TCRβ template counts to the total amount of DNA usable for TCR sequencing, where the amount of usable DNA was determined by PCR amplification and sequencing of housekeeping genes expected to be present in all nucleated cells. T-cell richness is a metric of T-cell diversity, and it was calculated by the T-cell unique rearrangements. T-cell clonality is a metric of T-cell proliferation and reactivity, and it was defined as 1 − Pielou evenness and was calculated on productive rearrangements by:

$$1 + \frac{\sum_{i}^{N} p_i \log_2(p_i)}{\log_2(N)}$$

where p_i is the proportional abundance of rearrangement i, and N is the total number of rearrangements. Clonality ranges from 0 to 1: values approaching 0 indicate a very even distribution of frequency of different clones (polyclonal), whereas values approaching 1 indicate a distinct asymmetric distribution, in which a few activated clones are present at high frequencies (monoclonal). Statistical analysis was performed in R version 3.2. Morisita index (MOI) is a measure of the similarity in the T-cell repertoire between samples ranging from 0 to 1, taking into account the specific rearrangements and their respective frequencies, with an MOI of 1 being an identical T-cell repertoire.

Statistical Analysis

Graphs were generated with GraphPad Prism 8.0. Spearman rank correlations were calculated to assess association between two continuous variables. Wilcoxon signed-rank test was applied to test the mutational burden, mutation concordance, SCNA burden, SCNA concordance, predicted neoantigens, neoantigen concordance, and TCR metrics over time, respectively. Mann–Whitney test was used to compare TCR metrics of MPM and NSCLC. Linear regression was used to model the relationship between TCR metrics and survival. Two-sided P values less than 0.05 were considered to be statistically significant.

Results

Homogenous mutational profiles between different tumor regions from the same MPM

A total of 5,021 nonsynonymous mutations (Supplementary Data) were detected in 69 tumor regions with a median total mutational burden (TMB) of 0.65/Mb, consistent with that from The Cancer Genome Atlas MPM cohort (ref. 31; 0.65/Mb; $P = 0.35$). The average TMB in tumors before dasatinib treatment was 0.65/Mb, similar with that of post-dasatinib treatment tumors (0.62/Mb; $P = 0.5$; Supplementary Fig. S1A). The median proportion of shared mutations between any pair of tumor regions was 80% (43%–90%) prior to and 83% (71%–88%) post-dasatinib treatment (**Fig. 1**). The average pairwise mutational concordance between any two regions of the same tumors in these nine patients with MPM was no different pre- and post-dasatinib treatment ($P = 0.3$; Supplementary Fig. S1B), suggesting that dasatinib treatment did not significantly change the mutational ITH complexity. We further predicted neoantigens from these somatic mutations, but did not observe significant changes in total predicted neoantigen burden or proportion of neoantigens shared by different regions within the same tumors before and after dasatinib treatment (Supplementary Figs. S2A and S2B and S3).

We next looked into a set of significantly mutated genes (SMG) identified from two large mesothelioma cohorts (31, 32) and found eight mutations in five SMGs (*BAP1, NF2, TP53, DDX3X*, and *RYR2*). All eight mutations were detected in both pretreatment and posttreatment tumors and six of the eight mutations were present in all regions within the same tumors (**Fig. 1**), suggesting these mutations may have been early genomic events during clonal evolution of these MPM tumors. However, two *NF2* mutations were heterogeneous mutations. A *NF2* stop-gain mutation was detected in both pretreatment specimens, but was missing in one of the posttreatment tumor specimens from patient M4, and a *NF2* nonsynonymous mutation (p.G123X) was identified in one of the three pretreatment tumor specimens and one of six posttreatment specimens from patient M11 suggesting these two *NF2* mutations may be later subclonal mutations in patients M4 and M11.

Mutations are predominantly driven by deficient DNA repair pathways

Understanding how mutational processes shape MPM evolution may inform mechanisms underlying tumor adaptation. We next calculated the contribution of different mutational signatures to investigate the mutational processes operative in this cohort of MPM. In 58 of 69 (84%) tumor specimens, COSMIC Signature 3 (associated with failure of DNA double-strand break repair by homologous recombination) or Signature 15 (associated with defective DNA mismatch repair) was most predominant (**Fig. 2**), suggesting that DNA repair deficiencies played a major role in mutagenesis in this cohort of MPM. The only exception was the tumor from patient M14, in which COSMIC Signature 4 (associated with cigarette smoking) and Signature 24 (with known exposures to aflatoxin) were the predominant signatures accounting for a median of 35% (2%–44%) and 25% (14%–33%), respectively.

Homogeneous SCNA profiles in MPM

SCNA is another key feature of human malignancies that could potentially impact expression of large groups of genes and SCNA ITH may have a profound impact on cancer biology and clinical outcome (16). Therefore, we next delineated the SCNA profiles and SCNA ITH architecture of this cohort of MPM. First, we calculated SCNA burden defined as the average number of genes with SCNA for each MPM specimen. As shown in Supplementary Fig. S4, although the SCNA burden varied substantially between different patients, it was very similar between different regions within the same tumors suggesting substantial interpatient heterogeneity, but limited ITH. Furthermore, no significant difference was observed in SCNA burden between tumors prior to versus post-dasatinib treatment (Supplementary Fig. S5A). We next measured concordance for SCNAs across multiple regions from the same tumors (either prior to or post-dasatinib treatment) as the surrogate for SCNA ITH. The average pairwise SCNA concordance between different regions of the same tumors was 0.83 (0.52–0.99) indicating homogenous SCNA ITH architecture in this cohort of MPM overall. In addition, dasatinib did not significantly change the SCNA concordance (Supplementary Fig. S5B). Furthermore, we investigated a list of cancer genes reported to be altered by SCNA in two large mesothelioma cohorts (31, 32). As shown in Supplementary Fig. S6, different regions within the same tumors showed a high level of homogeneity of SCNAs in cancer genes including deletions of *BAP1, CDKN2A* and an amplification of *NTRK3*.

Substantial T-cell repertoire heterogeneity in MPM

We previously demonstrated that a heterogeneous T-cell repertoire is associated with inferior clinical outcome in localized NSCLC (15). In this study, we performed multiregion TCR sequencing of 63 tumor

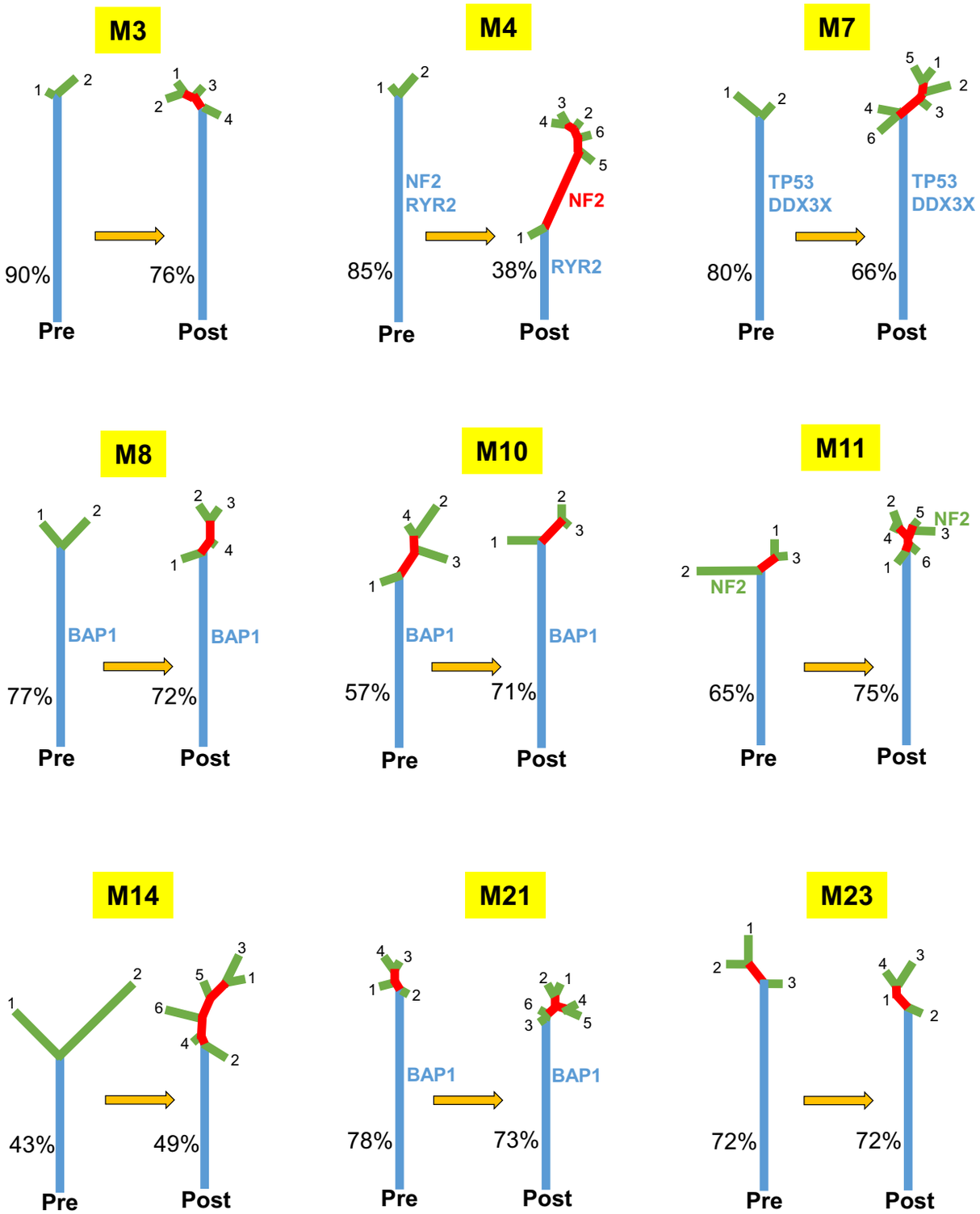

Figure 1.
Genomic ITH of nine MPM tumors before and after dasatinib treatment. Phylogenetic trees were generated from all mutations by Wagner parsimony method. The length of trunk (blue), branch (red), and private branches (green) is proportional to the number of mutations identified in all regions within the same tumor, some but not all regions, and only one single-tumor region, respectively. Pre: prior to dasatinib treatment; post: post-dasatinib treatment.

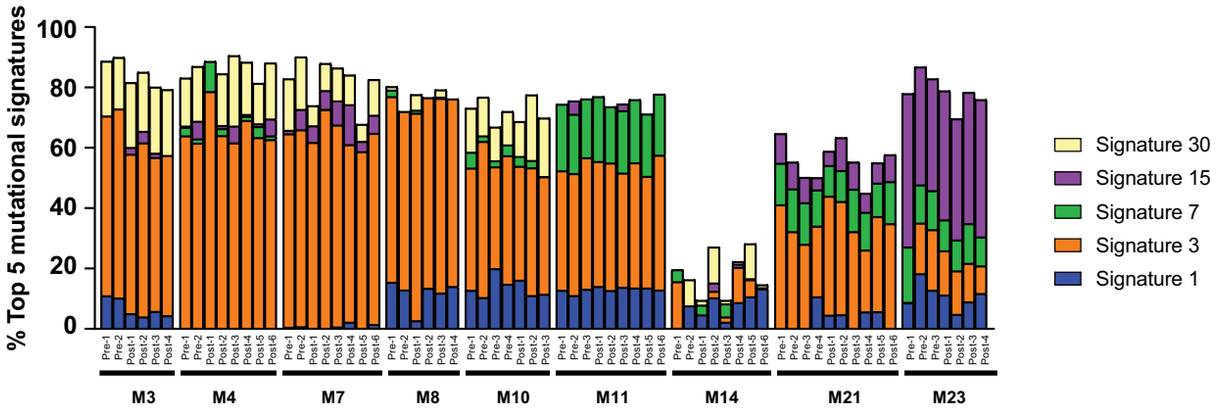

Figure 2.
The top five mutational signatures in MPM tumors. Pre: prior to dasatinib treatment; post: post-dasatinib treatment.

regions (two to six regions per tumor) from these nine patients with MPM with available DNA to depict the TCR repertoire and TCR ITH of this cohort of MPM, including 19 specimens from seven patients prior to dasatinib treatment and 44 posttreatment specimens from nine patients. In pretreatment tumors, T-cell density, an estimate of the proportion of T cells in a sample, ranged from 0.07 to 0.43 (average = 0.22) and richness, a measure of T-cell diversity, ranged from 2,189 to 11,568 (average = 5,946 unique rearrangements), which were comparable with localized NSCLC (ref. 30; Supplementary Fig. S7A and S7B). On the other hand, T-cell clonality, a parameter indicating T-cell expansion and reactivity, ranged from 0.04 to 0.14 (average = 0.08), was significantly lower than in localized NSCLC ($P = 0.0005$; ref. 30; Supplementary Fig. S7C). Interestingly, compared with pretreatment tumors, posttreatment MPM tumors exhibited similar T-cell density (average 0.22 vs. 0.22; $P > 0.99$) and richness (average 5,946 vs. 6,576; $P = 0.84$), but significantly increased T-cell clonality (average 0.08 vs. 0.13; $P = 0.047$ Supplementary Fig. S8A–S8C) suggesting expansion and activation of T cells post-dasatinib treatment.

To gain insights into spatial heterogeneity of T-cell response in MPM, we next investigated the overlap in T-cell clones across different regions from the same tumors. As shown in **Fig. 3A**, the vast majority (average, 82%; from 73% to 95%) of T-cell clones were restricted to individual tumor regions, while only an average of 6% (0.6%–19%) of T-cell clones were trunk TCR detectable across all tumor regions from the same tumors suggesting profound heterogeneity in T-cell response in this cohort of MPM. To comprehensively quantify the TCR ITH, we then utilized MOI, a metric taking into consideration not only the composition of T-cell clones but also the abundance of individual T-cell clones. MOI ranges from 0 to 1, with 1 indicating identical TCR repertoires and 0 indicating completely distinct TCR repertoires. The average MOI was 0.63 (ranging from 0.40 to 0.93) for this cohort of MPM (**Fig. 3B**), significantly lower than 0.82 (ranging from 0.61 to 0.93) in NSCLC ($P = 0.0097$; ref. 15; Supplementary Fig. S9).

Evolution of TCR repertoire after dasatinib treatment was associated with improved prognosis

Next, we attempted to assess whether the TCR ITH would impact clinical outcomes of these patients with MPM, although the sample size was small. With a median of 23.1 months of follow-up after surgical resection, all nine patients recurred and expired. Importantly, patients with higher T-cell clonality in post-dasatinib–treated MPM tumors had significantly longer OS (**Fig. 4A**) and a trend of longer progression-free survival (PFS; Supplementary Fig. S10A). In addition, the change of clonality after dasatinib treatment (posttreatment clonality – pretreatment clonality) was also associated with longer OS (**Fig. 4B**) and a trend of longer PFS (Supplementary Fig. S10B). Furthermore, patients with more homogenous TCR repertoire, indicated by higher proportion of trunk TCR detected in all tumor regions within the same tumors or higher MOI, in post-dasatinib–treated tumors demonstrated a trend of longer OS (**Fig. 4C** and **D**) and PFS (Supplementary Fig. S10C and S10D). Of note, neither PFS nor OS was associated with TCR parameters in pre-dasatinib treatment tumors. Taken together, these findings suggest that TCR expansion and activation, as well as homogeneous T-cell response after dasatinib treatment may impact patient outcome.

Discussion

ITH is increasingly recognized as a critical component of cancer biology that may have profound impact on outcome of patients with cancer (8, 13, 33). ITH could provide diverse genetic elements to foster tumor evolution along with tumor progression and/or during treatment leading to the selection of therapeutic-resistant cancer cell clones (34). By multiregion WES, we revealed relatively homogenous genomic ITH pattern in this cohort of MPM with the majority of mutations and SCNAs, including canonical cancer genes alterations, present across all the regions of the same MPM tumors. These findings were surprising for the following reasons. First, MPM grows in a unique pattern, wide spreading as an irregular pleural rind, which provides adequate space for different cancer clones to evolve in parallel, particularly without effective immune surveillance applying selection pressure, leading to more heterogeneous cancer cell populations. Second, the relatively low response rate to chemotherapy and high incidence of recurrence of MPM are attributed, in part, to a very high degree of molecular diversity within the tumor (35). One plausible explanation for the homogenous genomic landscape in MPM is that the majority of these mutations are very early molecular events during MPM evolution, which have had occurred before these tumors have spread locally. Our recent data in NSCLC have shown that nearly 70% mutations were shared even between primary tumors and distant metastases that developed several years later (36), suggesting that the majority of mutations have had occurred prior to distant metastases. Nevertheless, these data indicate that a single biopsy analysis

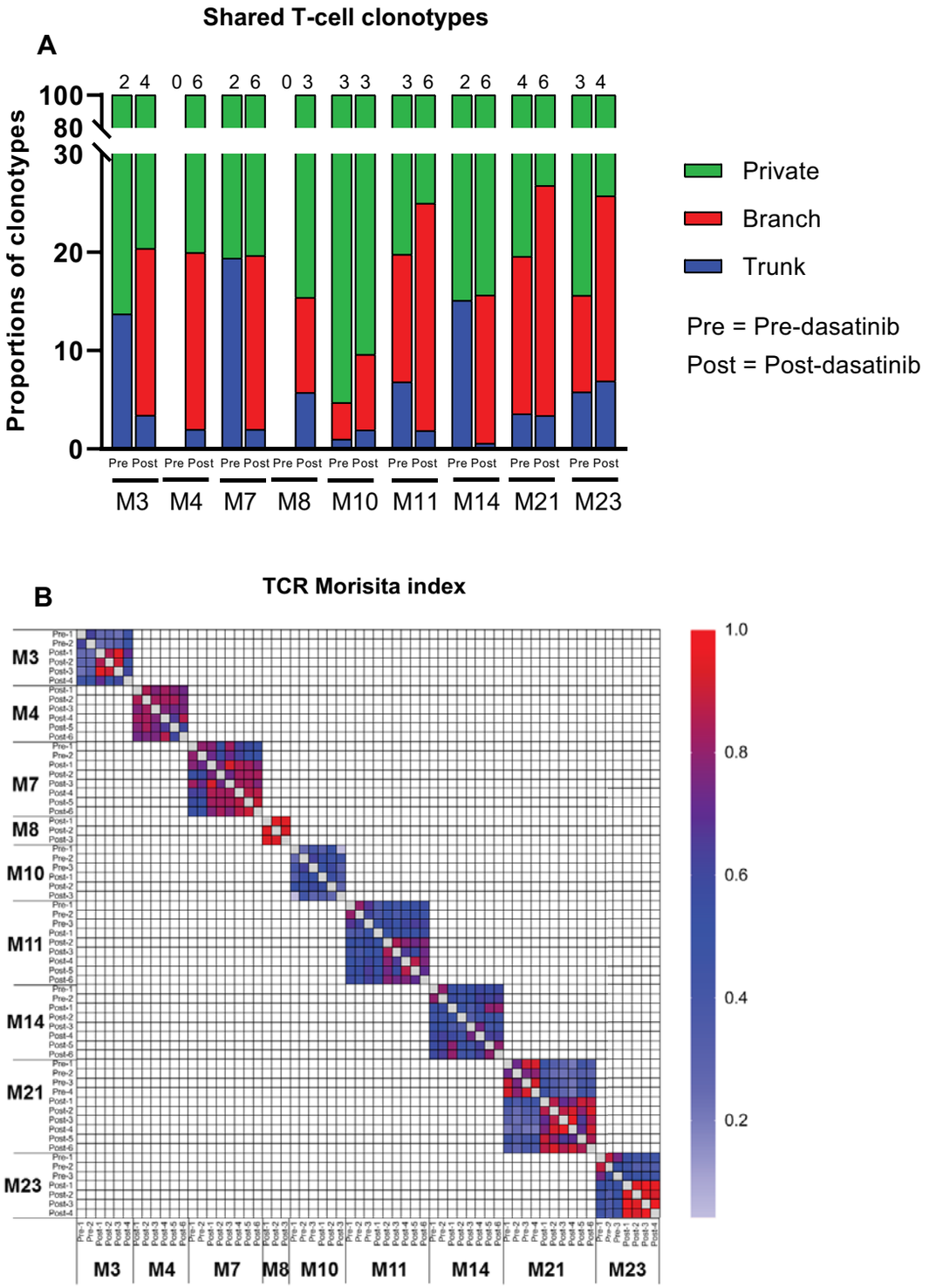

Figure 3.

T-cell repertoire ITH in MPM tumors. **A,** The proportions of T-cell clonotypes detected in all regions of tumors (trunk, blue), shared by at least two regions from the same tumors (branch, red), and restricted to a single region within the tumor (private, green). **B,** Quantification of TCR ITH by MOI, a metric taking into consideration the composition of T-cell clones and the abundance of individual T-cell clones between two samples. MOI ranges from 0 to 1, with 1 indicating identical TCR repertoires and 0 indicating completely distinct TCR repertoires. The color scales indicate the MOI between any two tumor regions. Pre: prior to dasatinib treatment; post: post-dasatinib treatment.

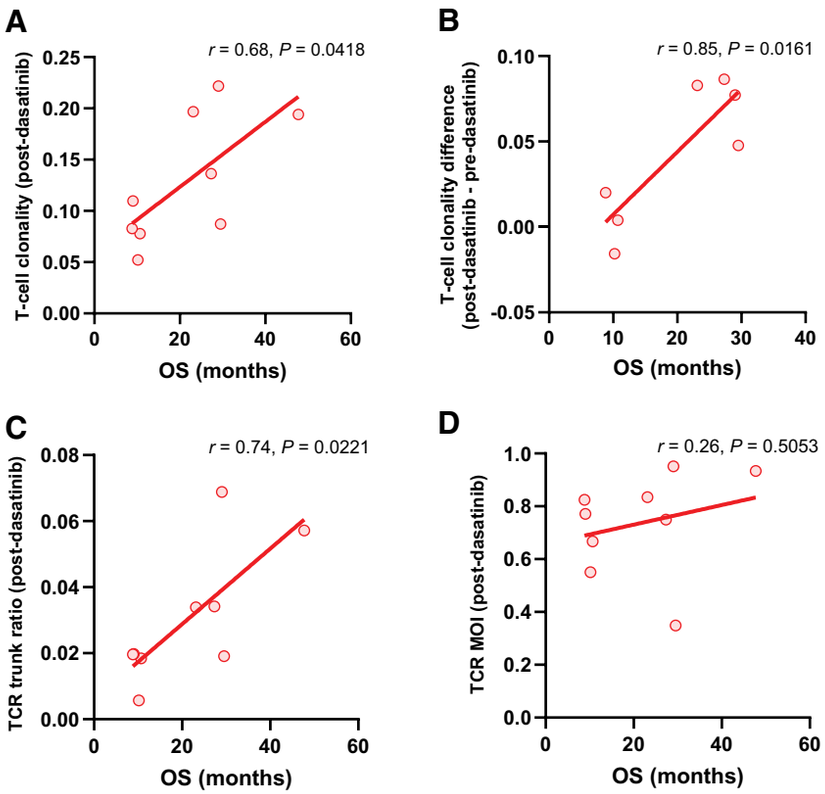

Figure 4.

TCR repertoire and TCR ITH in post-dasatinib–treated tumors were associated with OS. Correlation between OS and T-cell clonality (**A**), change of clonality post-dasatinib treatment (**B**), proportion of trunk TCR clonotypes detected in all tumor regions with the same tumors (**C**), and TCR MOI (**D**).

might be sufficient to identify the majority of known cancer gene mutations in MPM.

The tumor immune microenvironment, particularly, T-cell repertoire plays critical roles in determining cancer biology and clinical behaviors. Our study revealed for the first time the TCR repertoire features of MPM. Of particular interest, when compared with NSCLC, MPM has similar T-cell density and richness, but a significantly lower T-cell clonality, implying less T-cell expansion and activation in MPM. Furthermore, distinct T-cell repertoire in different tumor regions could also hamper effective antitumor immune response (15). Our multiregion TCR sequencing data have provided a unique opportunity to investigate T-cell repertoire ITH architecture within this cohort of MPM. The results have revealed profound TCR ITH with 73%–95% of all T-cell clones restricted to individual tumor regions. Importantly, the average MOI, a surrogate for comprehensive quantification of TCR ITH, was only 0.63, even significantly lower than NSCLC indicating a higher degree of TCR ITH in MPM.

The molecular mechanisms underlying the high TCR ITH in the background of homogeneous genomic landscape in MPM are beyond the scope of this study. There are several plausible reasons. For example, chromothripsis, a mutational process generating aberrant complex chromosomal rearrangements, is a critical mechanism underlying the evolution of malignant cell clones (37, 38). A recent study by Mansfield and colleagues (39) demonstrated that inter- or intrachromosomal rearrangements in a pattern of chromothripsis generated the junctions of genes and noncoding DNA with neoantigenic potential in MPM. Chromothripsis-like genome alterations could be heterogeneous and lead to vastly heterogenous neoantigen profiles in different regions of MPM and subsequent heterogeneous T-cell response. However, reliable detection of chromothripsis-like genome alterations requires whole-genome level data, while the limited exome-sequencing data in this study were not sufficient for this analysis. Moreover, other "heterogeneous" molecular changes (e.g., DNA methylation; ref. 18, acetylation, gene expression; ref. 17, and posttranslation modification) may exist contributing to the "heterogeneous" immune response. Furthermore, in addition to the tumors' intrinsic characteristics, immune landscape can also be altered by diverse extrinsic factors such as "bystander" T cells within tumors associated with local inflammation and viral infection (30). Future multi-omics studies incorporating comprehensive tumor features as well as relevant extrinsic factors are needed to better understand the molecular features underlying the extremely high TCR heterogeneity in MPM.

Nevertheless, the impaired T-cell expansion (low clonality) and profound TCR ITH (low MOI) may lead to an ineffective antitumor T-cell response, which could be one potential mechanism underlying the frequent recurrence of MPM. Moreover, although immune checkpoint blockade (ICB)-targeting T cells have revolutionized the therapeutic landscape across many different cancer types (40–46), the response rates to single-agent ICB treatment were only 9%–30% in patients with MPM (47–51). The suppressed and heterogeneous T-cell response in MPM may be one attributing factor for such suboptimal responses. As such, novel therapeutic strategies with or without ICB are warranted to improve the clinical outcome of patients with MPM.

We have previously conducted a neoadjuvant clinical trial using dasatinib in patients with resectable MPM (6, 20). Unfortunately, the clinical trial did not meet the primary endpoint (6). However, patients who had improved PFS with decreased p-Src^{Tyr419} post-dasatinib treatment, suggest dasatinib may benefit some patients with MPM. As a broad-spectrum tyrosine kinase inhibitor, dasatinib has been shown to modulate T-cell repertoire by reducing regulatory T-cell (Treg) populations while enhancing CD8^{+} antitumor T response (52, 53). In this study, we observed a significant increase

in T-cell clonality post-dasatinib treatment suggesting dasatinib may have induced T-cell expansion and activation. More importantly, regardless of small sample size, higher T-cell clonality in the post-treatment MPM specimens (not pretreatment specimens) and higher level of T-cell clonality increase after dasatinib treatment were associated with superior survival. Similarly, higher proportion of trunk TCR in post-dasatinib–treated specimens (but not pretreatment specimens), indicating more homogenous T-cell distribution after dasatinib treatment, was associated with superior survival. These results are in-line with previous findings that those molecular alterations from on-treatment biopsies were superior than pretreatment biopsies regarding the association with benefit from receiving ICB treatment in patients with melanoma (54). Because of the complexity of cancer biology and substantial interpatient heterogeneity, it is challenging to identify molecular features associated with therapeutic benefits in the pre-treatment biopsies. However, molecular changes reflecting the actual biological response to therapies from on-treatment biopsies may be a better predictor for clinical response. Although these on-treatment biopsy–based molecular changes are not desirable compared with pretreatment biopsy–based molecular features as potential biomarkers, they can be of value to discontinue ineffective treatment early during the disease course, particularly if these features are predictive of long-term benefit.

Our study has several important limitations. First, the sample size was small, which precluded us to make robust conclusions. Second, we did not have transcriptomic data to further dissect the ITH architecture, for example, distinct molecular subtypes (sarcomatoid, epithelioid, biphasic-epithelioid, and biphasic-sarcomatoid components; refs. 12, 32). Third, we did not have enough materials to depict the detailed immunologic features of these tumor-infiltrating T lymphocytes. However, our previous study on NSCLC has demonstrated that T-cell clonality was mainly driven by cytotoxic T lymphocytes and negatively regulated by Tregs (30), while MPM is known to be enrich for immunosuppressive and anergic immune cells, such as Tregs, monocytic myeloid-derived suppressor cells (Gr-MDSC/Mo-MDSC), and M2-polarized tumor-associated macrophages (55–59), in-line with suppressed T-cell repertoire observed in this study.

With all the above limitations fully acknowledged, the multiregional, paired longitudinal specimens before and posttreatment from a rare and aggressive malignancy made the data invaluable. In summary, we demonstrated that despite the homogeneous genomic landscape, MPM has a suppressed and extremely heterogeneous TCR repertoire. This may lead to ineffective host antitumor immune surveillance, which could be one potential molecular mechanism underlying high recurrence rate and suboptimal response to immunotherapy in MPM. Future studies are warranted to combine ICB with novel agents that have the potential to induce T-cell activation, such as dasatinib, to improve the clinical outcome of patients with MPM.

Disclosure of Potential Conflicts of Interest

S.G. Swisher reports personal fees from Egyptian Society of Surgical Oncology (speaker) and West Hawaii Symposium (speaker) and other from Ethicon (scientific advisory committee member/no compensation) outside the submitted work, and reports patent number 62802957, Compounds and Methods for the Treatment of PKR-Associated Diseases owned by The University of Texas System. B. Sepesi reports personal fees from Bristol Myers Squib outside the submitted work. H.T. Tran reports grants from Guardant Health Inc (research) and BAYER AS (research) outside the submitted work. J.V. Heymach reports personal fees from BMS (scientific advisory board, research support) during the conduct of the study, as well as personal fees from Boehringer Ingelheim (scientific advisory board), EMD Serono (scientific advisory board), Lilly (scientific advisory Board), Foundation Medicine (scientific advisory board), Hengrui Therapeutics (scientific advisory board), Guardant Health (scientific advisory board), Merck (scientific advisory board), Novartis (scientific advisory board), Pfizer (scientific advisory board), Genentech/Roche (scientific advisory board), Takeda (scientific advisory board), and Sanofi (scientific advisory board), and grants and personal fees from AstraZeneca (scientific advisory board, research support), GlaxoSmithKline (scientific advisory board, research support), and Spectrum (scientific advisory board, research support, licensing fees) outside the submitted work. I.I. Wistuba reports grants and personal fees from Genentech/Roche, Bayer, Bristol-Myers Squibb, Pfizer, HTG Molecular, Asuragen, Merck, and Guardant Health, personal fees from Oncocyte, GlaxoSmithKline, MSD, and PlatformQ Health, and grants from OncoPLEX, DEPArray, AstraZeneca/Medimmune, Adaptive, Adaptimmune, EMD Serono, Takeda, Amgen, Karus, Johnson & Johnson, Iovance, 4D, Novartis, and Akoya outside the submitted work. A. Tsao was on the advisory board for Genentech, EMD Serono, Merck, BMS, Eli Lilly, Roche, Novartis, Ariad, Seattle Genetics, AstraZeneca, Boehringer-Ingelheim, Sellas Life Science, and Takeda; received grants from Millennium, Polaris, Epizyme, EMD Serono, and Seattle Genetics outside the submitted work. J. Zhang reports grants from Merck, grants and personal fees from Johnson and Johnson, and personal fees from Geneplus-Beijing Institute, BMS, OrigMed, AstraZeneca, and Innovent outside the submitted work. No potential conflicts of interest were disclosed by the other authors.

Authors' Contributions

R. Chen: Data curation, formal analysis, validation, investigation, methodology, writing-original draft, writing-review and editing. **W.-C. Lee:** Data curation, validation, investigation, methodology, writing-original draft, writing-review and editing. **J. Fujimoto:** Data curation, methodology. **J. Li:** Methodology. **X. Hu:** Methodology. **R. Mehran:** Data curation, methodology. **D. Rice:** Data curation, methodology. **S.G. Swisher:** Data curation, methodology. **B. Sepesi:** Data curation, methodology. **H.T. Tran:** Investigation. **C.-W. Chow:** Methodology. **L.D. Little:** Methodology. **C. Gumbs:** Methodology. **C. Haymaker:** Data curation, methodology. **J.V. Heymach:** Data curation, investigation. **I.I. Wistuba:** Data curation, investigation, methodology. **J.J. Lee:** Methodology, writing-review and editing. **P.A. Futreal:** Resources, supervision, funding acquisition, investigation, methodology. **J. Zhang:** Resources, data curation, investigation, methodology. **A. Reuben:** Supervision, investigation, writing-review and editing. **A.S. Tsao:** Conceptualization, resources, data curation, supervision, investigation, writing-review and editing. **J. Zhang:** Conceptualization, resources, supervision, funding acquisition, writing-review and editing.

Acknowledgments

This study was supported by Conquer Cancer Foundation ASCO Young Investigator Award, MD Anderson Physician Scientist Award, University Cancer Foundation Sister Institution Network Fund, Cancer Prevention & Research Institute of Texas Multiple Investigator Award, TJ Martell Foundation, Aileen M. Dillon and Lee M. Bourg Mesothelioma Fund, and Ronald E. and Reba M. Kennedy Endowment for Lung Cancer Research.

The costs of publication of this article were defrayed in part by the payment of page charges. This article must therefore be hereby marked *advertisement* in accordance with 18 U.S.C. Section 1734 solely to indicate this fact.

Received May 6, 2020; revised June 30, 2020; accepted August 5, 2020; published first August 14, 2020.

References

1. Nelson DB, Rice DC, Niu J, Atay SM, Vaporciyan AA, Antonoff MB, et al. Predictors of trimodality therapy and trends in therapy for malignant pleural mesothelioma. Eur J Cardiothorac Surg 2018;53:960–6.

2. Carbone M, Adusumilli PS, Alexander HR Jr, Baas P, Bardelli F, Bononi A, et al. Mesothelioma: scientific clues for prevention, diagnosis, and therapy. CA Cancer J Clin 2019;69:402–29.

3. Carbone M, Yang H, Pass HI, Krausz T, Testa JR, Gaudino G. BAP1 and cancer. Nat Rev Cancer 2013;13:153–9.
4. Pastorino S, Yoshikawa Y, Pass HI, Emi M, Nasu M, Pagano I, et al. A subset of mesotheliomas with improved survival occurring in carriers of BAP1 and other germline mutations. J Clin Oncol 2018;36:3485–94.
5. Alpert N, van Gerwen M, Taioli E. Epidemiology of mesothelioma in the 21st century in Europe and the United States, 40 years after restricted/banned asbestos use. Transl Lung Cancer Res 2020;9:S28–S38.
6. Tsao AS, Lin H, Carter BW, Lee JJ, Rice D, Vaporcyan A, et al. Biomarker-integrated neoadjuvant dasatinib trial in resectable malignant pleural mesothelioma. J Thorac Oncol 2018;13:246–57.
7. Mutti L, Peikert T, Robinson BWS, Scherpereel A, Tsao AS, de Perrot M, et al. Scientific advances and new frontiers in mesothelioma therapeutics. J Thorac Oncol 2018;13:1269–83.
8. Yap TA, Gerlinger M, Futreal PA, Pusztai L, Swanton C. Intratumor heterogeneity: seeing the wood for the trees. Sci Transl Med 2012;4:127ps10.
9. Swanton C. Intratumor heterogeneity: evolution through space and time. Cancer Res 2012;72:4875–82.
10. Fisher R, Pusztai L, Swanton C. Cancer heterogeneity: implications for targeted therapeutics. Br J Cancer 2013;108:479–85.
11. Gerlinger M, Horswell S, Larkin J, Rowan AJ, Salm MP, Varela I, et al. Genomic architecture and evolution of clear cell renal cell carcinomas defined by multiregion sequencing. Nat Genet 2014;46:225–233.
12. Blum Y, Meiller C, Quetel L, Elarouci N, Ayadi M, Tashtanbaeva D, et al. Dissecting heterogeneity in malignant pleural mesothelioma through histo-molecular gradients for clinical applications. Nat Commun 2019;10:1333.
13. Gerlinger M, Rowan AJ, Horswell S, Larkin J, Endesfelder D, Gronroos E, et al. Intratumor heterogeneity and branched evolution revealed by multiregion sequencing. N Engl J Med 2012;366:883–92.
14. Zhang J, Fujimoto J, Zhang J, Wedge DC, Song X, Zhang J, et al. Intratumor heterogeneity in localized lung adenocarcinomas delineated by multiregion sequencing. Science 2014;346:256–9.
15. Reuben A, Gittelman R, Gao J, Zhang J, Yusko EC, Wu C-J, et al. TCR repertoire intratumor heterogeneity in localized lung adenocarcinomas: an association with predicted neoantigen heterogeneity and postsurgical recurrence. Cancer Discov 2017;7:1088–97.
16. Jamal-Hanjani M, Wilson GA, McGranahan N, Birkbak NJ, Watkins TBK, Veeriah S, et al. Tracking the evolution of non-small-cell lung cancer. N Engl J Med 2017;376:2109–21.
17. Lee WC, Diao L, Wang J, Zhang J, Roarty EB, Varghese S, et al. Multiregion gene expression profiling reveals heterogeneity in molecular subtypes and immunotherapy response signatures in lung cancer. Mod Pathol 2018;31:947–55.
18. Quek K, Li J, Estecio M, Zhang J, Fujimoto J, Roarty E, et al. DNA methylation intratumor heterogeneity in localized lung adenocarcinomas. Oncotarget 2017;8:21994–2002.
19. Rosenthal R, Cadieux EL, Salgado R, Bakir MA, Moore DA, Hiley CT, et al. Neoantigen-directed immune escape in lung cancer evolution. Nature 2019;567:479–85.
20. Tsao AS, He D, Saigal B, Liu S, Lee JJ, Bakkannagari S, et al. Inhibition of c-Src expression and activation in malignant pleural mesothelioma tissues leads to apoptosis, cell cycle arrest, and decreased migration and invasion. Mol Cancer Ther 2007;6:1962–72.
21. Cibulskis K, Lawrence MS, Carter SL, Sivachenko A, Jaffe D, Sougnez C, et al. Sensitive detection of somatic point mutations in impure and heterogeneous cancer samples. Nat Biotechnol 2013;31:213–9.
22. Ye K, Schulz MH, Long Q, Apweiler R, Ning ZM. Pindel: a pattern growth approach to detect break points of large deletions and medium sized insertions from paired-end short reads. Bioinformatics 2009;25:2865–71.
23. Rosenthal R, McGranahan N, Herrero J, Taylor BS, Swanton C. DeconstructSigs: delineating mutational processes in single tumors distinguishes DNA repair deficiencies and patterns of carcinoma evolution. Genome Biol 2016;17:31.
24. Ha G, Roth A, Lai D, Bashashati A, Ding J, Goya R, et al. Integrative analysis of genome-wide loss of heterozygosity and monoallelic expression at nucleotide resolution reveals disrupted pathways in triple-negative breast cancer. Genome Res 2012;22:1995–2007.
25. Zhang J. CNTools: convert segment data into a region by sample matrix to allow for other high level computational analyses. R package (version 16 0). http://bioconductor.org/packages/release/bioc/html/CNTools.html.
26. Grasso C, Butler T, Rhodes K, Quist M, Neff TL, Moore S, et al. Assessing copy number alterations in targeted, amplicon-based next-generation sequencing data. J Mol Diagn 2015;17:53–63.
27. Favero F, Joshi T, Marquard AM, Birkbak NJ, Krzystanek M, Li Q, et al. Sequenza: allele-specific copy number and mutation profiles from tumor sequencing data. Ann Oncol 2015;26:64–70.
28. Schenck RO, Lakatos E, Gatenbee C, Graham TA, Anderson AR. NeoPredPipe: high-throughput neoantigen prediction and recognition potential pipeline. BMC Bioinformatics 2019;20:264.
29. Nariai N, Kojima K, Saito S, Mimori T, Sato Y, Kawai Y, et al. HLA-VBSeq: accurate HLA typing at full resolution from whole-genome sequencing data. BMC Genomics 2015;16:S7.
30. Reuben A, Zhang J, Chiou SH, Gittelman RM, Li J, Lee WC, et al. Comprehensive T cell repertoire characterization of non-small cell lung cancer. Nat Commun 2020;11:603.
31. Hmeljak J, Sanchez-Vega F, Hoadley KA, Shih J, Stewart C, Heiman D, et al. Integrative molecular characterization of malignant pleural mesothelioma. Cancer Discov 2018;8:1548–65.
32. Bueno R, Stawiski EW, Goldstein LD, Durinck S, De Rienzo A, Modrusan Z, et al. Comprehensive genomic analysis of malignant pleural mesothelioma identifies recurrent mutations, gene fusions and splicing alterations. Nat Genet 2016;48:407–16.
33. McGranahan N, Swanton C. Clonal heterogeneity and tumor evolution: past, present, and the future. Cell 2017;168:613–28.
34. McGranahan N, Swanton C.. Biological and therapeutic impact of intratumor heterogeneity in cancer evolution. Cancer Cell 2015;27:15–26.
35. Oehl K, Vrugt B, Opitz I, Meerang M. Heterogeneity in malignant pleural mesothelioma. Int J Mol Sci 2018;19:1603.
36. Lee W-C, Gomez D, Zhang J, Reuben A, Jalali A, Roh W, et al. Abstract 2741: comprehensive molecular profiling of primary tumors and paired distant metastases in non-small cell lung cancer. Cancer Res 2019;79:2741.
37. Ly P, Cleveland DW. Rebuilding chromosomes after catastrophe: emerging mechanisms of chromothripsis. Trends Cell Biol 2017;27:917–30.
38. Yoshikawa Y, Emi M, Hashimoto-Tamaoki T, Ohmuraya M, Sato A, Tsujimura T, et al. High-density array-CGH with targeted NGS unmask multiple noncontiguous minute deletions on chromosome 3p21 in mesothelioma. Proc Natl Acad Sci U S A 2016;113:13432–7.
39. Mansfield AS, Peikert T, Smadbeck JB, Udell JBM, Garcia-Rivera E, Elsbernd L, et al. Neoantigenic potential of complex chromosomal rearrangements in mesothelioma. J Thorac Oncol 2019;14:276–87.
40. Postow MA, Callahan MK, Wolchok JD. Immune checkpoint blockade in cancer therapy. J Clin Oncol 2015;33:1974.
41. Brahmer J, Reckamp KL, Baas P, Crino L, Eberhardt WE, Poddubskaya E, et al. Nivolumab versus docetaxel in advanced squamous-cell non-small-cell lung cancer. N Engl J Med 2015;373:123–35.
42. Borghaei H, Paz-Ares L, Horn L, Spigel DR, Steins M, Ready NE, et al. Nivolumab versus docetaxel in advanced nonsquamous non-small-cell lung cancer. N Engl J Med 2015;373:1627–39.
43. Herbst RS, Baas P, Kim DW, Felip E, Perez-Gracia JL, Han JY, et al. Pembrolizumab versus docetaxel for previously treated, PD-L1-positive, advanced non-small-cell lung cancer (KEYNOTE-010): a randomised controlled trial. Lancet 2016;387:1540–50.
44. Rittmeyer A, Barlesi F, Waterkamp D, Park K, Ciardiello F, von Pawel J, et al. Atezolizumab versus docetaxel in patients with previously treated non-small-cell lung cancer (OAK): a phase 3, open-label, multicentre randomised controlled trial. Lancet 2017;389:255–65.
45. Larkin J, Hodi FS, Wolchok JD. Combined nivolumab and ipilimumab or monotherapy in untreated melanoma. N Engl J Med 2015;373:1270–1.
46. Forde PM, Chaft JE, Smith KN, Anagnostou V, Cottrell TR, Hellmann MD, et al. Neoadjuvant PD-1 blockade in resectable lung cancer. N Engl J Med 2018;378:1976–86.
47. Okada M, Kijima T, Aoe K, Kato T, Fujimoto N, Nakagawa K, et al. Clinical efficacy and safety of nivolumab: results of a multicenter, open-label, single-arm, Japanese phase II study in malignant pleural mesothelioma (MERIT). Clin Cancer Res 2019;25:5485–92.
48. Alley EW, Lopez J, Santoro A, Morosky A, Saraf S, Piperdi B, et al. Clinical safety and activity of pembrolizumab in patients with malignant pleural mesothelioma (KEYNOTE-028): preliminary results from a non-randomised, open-label, phase 1b trial. Lancet Oncol 2017;18:623–30.
49. Quispel-Janssen J, van der Noort V, de Vries JF, Zimmerman M, Lalezari F, Thunnissen E, et al. Programmed death 1 blockade with nivolumab in patients with recurrent malignant pleural mesothelioma. J Thorac Oncol 2018;13:1569–76.

50. Hassan R, Thomas A, Nemunaitis JJ, Patel MR, Bennouna J, Chen FL, et al. Efficacy and safety of avelumab treatment in patients with advanced unresectable mesothelioma: phase 1b results from the JAVELIN solid tumor trial. JAMA Oncol 2019;5:351–7.
51. Mansfield AS.Immune checkpoint inhibition in malignant mesothelioma: does it have a future? Lung Cancer 2017;105:49–51.
52. Tan C-S, Kumarakulasinghe NB, Huang Y-Q, Ang YLE, Choo JR-E, Goh B-C, et al. Third generation EGFR TKIs: current data and future directions. Mol Cancer 2018;17:29.
53. Yang Y, Liu C, Peng W, Lizee G, Overwijk WW, Liu Y, et al. Antitumor T-cell responses contribute to the effects of dasatinib on c-KIT mutant murine mastocytoma and are potentiated by anti-OX40. Blood 2012;120:4533–43.
54. Chen PL, Roh W, Reuben A, Cooper ZA, Spencer CN, Prieto PA, et al. Analysis of immune signatures in longitudinal tumor samples yields insight into biomarkers of response and mechanisms of resistance to immune checkpoint blockade. Cancer Discov 2016;6:827–37.
55. Awad MM, Jones RE, Liu H, Lizotte PH, Ivanova EV, Kulkarni M, et al. Cytotoxic T cells in PD-L1–positive malignant pleural mesotheliomas are counterbalanced by distinct immunosuppressive factors. Cancer Immunol Res 2016;4:1038–48.
56. Khanna S, Graef S, Mussai F, Thomas A, Wali N, Yenidunya BG, et al. Tumor-derived GM-CSF promotes granulocyte immunosuppression in mesothelioma patients. Clin Cancer Res 2018;24:2859–72.
57. Hegmans JP, Hemmes A, Hammad H, Boon L, Hoogsteden HC, Lambrecht BN. Mesothelioma environment comprises cytokines and T-regulatory cells that suppress immune responses. Eur Respir J 2006;27:1086–95.
58. Cornelissen R, Lievense LA, Maat AP, Hendriks RW, Hoogsteden HC, Bogers AJ, et al. Ratio of intratumoral macrophage phenotypes is a prognostic factor in epithelioid malignant pleural mesothelioma. PloS One 2014;9:e106742.
59. Salaroglio IC, Kopecka J, Napoli F, Pradotto M, Maletta F, Costardi L, et al. Potential diagnostic and prognostic role of microenvironment in malignant pleural mesothelioma. J Thorac Oncol 2019;14:1458–71.